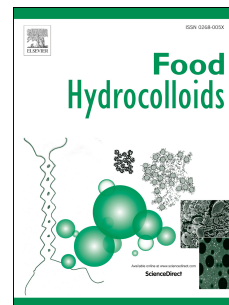# Accepted Manuscript

Superabsorbent food packaging bioactive cellulose-based aerogels from *Arundo donax* waste biomass

Cynthia Fontes, Evrim Erboz, Antonio Martínez-Abad, Amparo López-Rubio, Marta Martínez-Sanz

Please cite this article as: Fontes, C., Erboz, E., Martínez-Abad, A., López-Rubio, A., Martínez-Sanz, M., Superabsorbent food packaging bioactive cellulose-based aerogels from *Arundo donax* waste biomass, *Food Hydrocolloids* (2019), doi: https://doi.org/10.1016/j.foodhyd.2019.05.011.

1 **SUPERABSORBENT FOOD PACKAGING BIOACTIVE CELLULOSE-**

2 **BASED AEROGELS FROM *Arundo donax* WASTE BIOMASS**

3

4 Cynthia Fontes[1], Evrim Erboz[1], Antonio Martínez-Abad[2], Amparo López-Rubio[1] and

5 Marta Martínez-Sanz[1*]

6
7

8 [1]Food Safety and Preservation Department, IATA-CSIC, Avda. Agustín Escardino 7,

9 46980 Paterna, Valencia, Spain

10

11 [2]Dept. Analytical Chemistry, Nutrition and Food Sciences, University of Alicante,
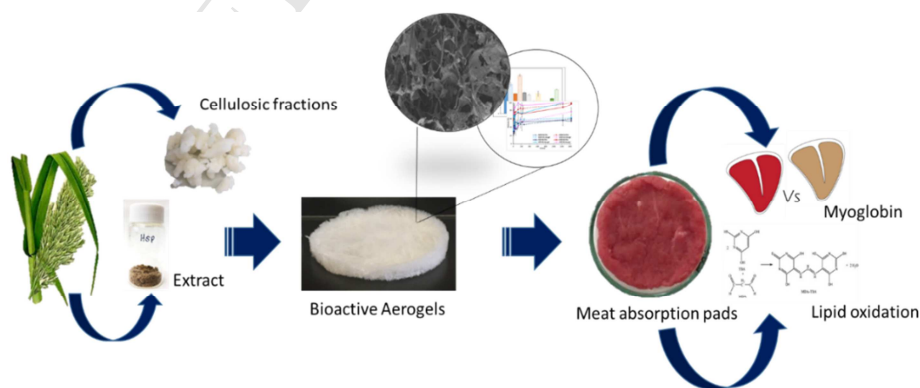
12 03690, San Vicente del Raspeig, Alicante, Spain

13

14 *Corresponding author: Tel.: +34 963200022; fax: +34 963636301

15 E-mail address: mmartinez@iata.csic.es

16

17

18

19

20

Abstract

A. donax waste biomass has been valorized for the extraction of cellulosic fractions with different purification degrees, as well as aqueous bioactive extracts, which were then combined to develop superabsorbent bioactive aerogels. All the developed aerogels presented excellent water and oil sorption capacities; however, the presence of hemicelluloses yielded more porous and hydrophilic aerogels, capable of absorbing more water. With regards to the aqueous extracts, the hot water treatment (HW) of *A. donax* stems promoted the extraction of polysaccharides and polyphenols, producing the extract (S-HW) with the highest antioxidant capacity. This extract was then incorporated into the aerogels produced from the less purified stem fractions (F2A and F3A), which were chosen due to their good water sorption capacity, higher antioxidant potential and lower production costs and environmental impact. The hybrid aerogels showed a great potential to be used as bioactive pads for food packaging. In particular, the F2A+S-HW aerogel would be the most optimum choice since it provides a complete release of the extract in hydrophilic media, as demonstrated by *in-vitro* release and β-carotene bleaching inhibition studies, and it is able to reduce the colour loss and lipid oxidation in red meat upon refrigerated storage to a greater extent.

1. Introduction

47   In the context of the extremely demanding market within the food industry,

48   packaging plays a crucial role, not only protecting the product from the external

49   environment and maintaining food quality to extend products' shelf life, but also

50   being able to provide added functionalities, such as the incorporation of health-

51   beneficial compounds (e.g. antioxidants) which can improve the nutritional value of

52   the packaged product. Accordingly, strategies based on the controlled release of

53   bioactive compounds from the package towards the food product, are being

54   extensively investigated. For instance, some studies have reported on the

55   incorporation of bioactive extracts into packaging films to preserve meat quality and

56   organoleptic properties (Barbosa-Pereira, Aurrekoetxea, Angulo, Paseiro-Losada, &

57   Cruz, 2014; Bolumar, Andersen, & Orlien, 2011; Camo, Lorés, Djenane, Beltrán, &

58   Roncalés, 2011; Jofré, Aymerich, & Garriga, 2008; Lorenzo, Batlle, & Gómez,

59   2014), demonstrating that the processes of lipid oxidation and colour loss upon

60   storage could be reduced through the antioxidant activity of the incorporated

61   extracts.

62   In the particular case of meat packaging, absorption pads are commonly used as

63   moisture control elements, which absorb the excess liquids released by meat upon

64   storage. These pads are typically made of a non-permeable/non-stick synthetic

65   polymer, such as polyethylene and a hydrophilic non-woven bottom layer filled with

66   active substances which prevent bacterial growth, such as citric acid and sodium

67   bicarbonate (McMillin, 2017). Given the severe environmental issues associated to

3

68 the production and use of synthetic plastics, current trends in the food packaging

69 sector are clearly moving towards the utilization of more sustainable bio-based and

70 renewable materials, i.e. biopolymers. Polysaccharides and, in particular,

71 lignocellulosic materials, have already demonstrated their great potential to develop

72 high performance bio-based packaging structures (Benito-González, López-Rubio, &

73 Martínez-Sanz, 2018; Martínez-Sanz, Erboz, Fontes, & López-Rubio, 2018;

74 Rampazzo et al., 2017; Satyanarayana, Arizaga, & Wypych, 2009). Lignocellulosic

75 materials can be extracted from multiple sources such as terrestrial and aquatic

76 plants, algae and agriculture and forestry-derived waste by-products (Trache, Hussin,

77 Haafiz, & Thakur, 2017). However, the extraction from waste or underutilized

78 resources that do not compete with the food chain is particularly interesting and in

79 line with the principles of circular economy. For instance, lignocellulosic fractions

80 have been extracted from waste biomass derived from the aquatic plant *Posidonia*

81 *oceanica* (Benito-González et al., 2018) and the aquatic invasive species *Arundo*

82 *donax* (Martínez-Sanz et al., 2018).

83

84 In addition to other polysaccharides, cellulosic materials have been used to produce

85 aerogel structures, which are extremely light, highly porous materials, with low

86 density, large surface area and high water sorption capacity (Henschen, Illergård,

87 Larsson, Ek, & Wågberg, 2016; Lin et al., 2014; Wang et al., 2016). Due to their

88 large inner surface areas and high surface-to-volume ratios, these aerogels may be

89 suitable for the development of controlled release systems. In fact, cellulose aerogels

90 from different vegetal and bacterial sources have already demonstrated their potential

91 as templates for the incorporation and sustained release of drugs (Haimer et al., 2010;

4

92 Valo et al., 2013), although their application in the food area has not been evaluated

93 yet. One of the issues associated to the production of cellulose aerogels is that they

94 are typically obtained by means of a complex synthesis method involving multiple

95 steps: (i) dissolution of cellulose through the disruption of its crystalline structure,

96 (ii) gelation, (iii) cellulose regeneration, (iv) solvent exchange and (v) a final drying

97 step such as freeze-drying or supercritical drying (Gavillon & Budtova, 2007;

98 Innerlohinger, Weber, & Kraft, 2006). Such process presents two main drawbacks:

99 the high production costs and the unsuitability of the produced aerogels for food-

100 grade applications due to the use of organic solvents.

101

102 In this work, the possibility of producing cellulose-based aerogels using a simple

103 freeze-drying method from aqueous suspensions of cellulosic fractions from *A.*

104 *donax* waste biomass with different purification degrees has been explored. To

105 further valorize this waste biomass, aqueous extracts were produced by simple

106 heating and ultrasound protocols and their composition and antioxidant capacity was

107 evaluated. Finally, the most active extract was incorporated into selected aerogels to

108 investigate the extract release and the antioxidant capacity of the hybrid structures, as

109 well as to evaluate them as bioactive superabsorbent pads to preserve the quality of

110 packaged red meat by reducing colour loss and lipid oxidation processes.

111

112 **2. Materials and Methods**

113 **2.1 Materials**

114 *Arundo donax* (*A. donax*) was collected from a freshwater environment in Buñol,

115 Valencia (Spain) in September 2017. The leaves were separated from the stems and

116   the material was washed vigorously with water, ground with an electric blender and

117   stored at 4 °C until use.

118   Gallic acid (97.5-102.5%), hydrochloric acid (37%), sulphuric acid (≥97.5%),

119   potassium sulphate, potassium persulphate (≥99%), potassium chloride (99%),

120   phosphate buffered saline tablets, ABTS (≥98%) and 6-hydroxy-2,5,7,8- tetramethyl

121   chroman-2-carboxylic acid (97%), β- carotene (≥97%), linoleic acid (≥99%),

122   Tween® 40, 2-Thiobarbituric acid (98%), ethylenediaminetetraacetic acid disodium

123   salt dehydrate (98.5-101.5%), propyl gallate, were obtained from Sigma-Aldrich

124   (Spain). Sodium chlorite 80% was obtained from Acros organics (Spain). The Folin-

125   Ciocalteau reagent, modified Lowry reagent and bovine serum albumin were

126   obtained from the "modified Lowry protein assay kit" purchased from Thermo Fisher

127   scientific (Spain).

128

129   **2.2 Preparation of holocellulosic fractions**

130   A purification procedure previously reported (Martínez-Sanz et al., 2018) for the

131   extraction of holocellulosic fractions from *A. donax* leaves and stems was applied,

132   generating six different fractions labelled as F2, F3, F2A, F3A, F2L and F3L.

133   Briefly, the stem biomass was subjected to a Soxhlet treatment, followed by a de-

134   lignification step with NaClO$_2$, obtaining F2. After that, the hemicelluloses were

135   removed by means of alkali treatment with KOH, yielding F3. The same process, but

136   omitting the initial Soxhlet treatment, was carried out to produce the fractions

137   labelled as F2A and F3A (obtained from the stem biomass) and F2L and F3L

138   (obtained from the leaf biomass). The obtained fractions were stored in the fridge as

139   partially hydrated materials until use.

6

140

2.3 Production of water-soluble extracts from *Arundo donax*

Water-soluble extracts were generated from *A. donax* leaves and stems, using two

different methods: (i) Hot water extraction (HW) and (ii) ultrasound-assisted

extraction (US).

For the hot water extraction, 10 g of leaf or stem biomass (dry weight basis) were

added to 200 mL of distilled water and mixed in a blender until a paste was obtained.

The material was then heated up to 90 ℃ and kept at a constant temperature and

under stirring for 1 h. After that, the material was centrifuged at 12500 rpm and 15℃

for 20 min. The supernatant was separated, placed in an ice bath and the required

volume of ethanol (75% with regards to the volume of aqueous supernatant v/v) was

slowly added. The material was kept stirring in the ice bath overnight and after that,

centrifuged again (12500 rpm, 15℃, 20 min). The precipitate was collected, re-

suspended in distilled water and freeze-dried. The obtained powder extracts were

labelled as S-HW (stem biomass) and L-HW (leaf biomass).

For the ultrasound-assisted extraction, 10 g of leaf or stem biomass (dry weight

basis) were added to 200 mL of distilled water, mixed in a blender and subjected to

an ultrasound treatment with a probe UP-400S (Hielcher GmbH, Germany) operating

at a maximum power of 400W and a constant frequency of 24 kHz for 30min. After

that, the material was centrifuged (12500 rpm, 15℃, 20 min) and processed

following the same procedure described for the hot water extraction. The obtained

powder extracts were labelled as S-US (stem biomass) and L-US (leaf biomass).

All the extracts were stored at 0% RH until further use.

163

2.4 Preparation of aerogels

Pure cellulosic aerogels were prepared by adding 0.075 g of the different fractions (dry weight) to 15 mL of distilled water and dispersing them by ultra-turrax homogenization until obtaining homogeneous suspensions. These were then poured into Petri dishes (diameter of 6 cm), frozen at -80 °C and subsequently, freeze-dried using a Genesis 35-EL freeze-dryer (Virtis). For the production of bioactive aerogels, 0.015 g of water-soluble extract (ca. 17 wt.-% with regards to the total solids content) were dispersed together with the corresponding lignocellulosic fraction. In order to assess the effect of the material porosity the same formulations used to produce the bioactive aerogels were utilized to generate films by a vacuum filtration method, as previously described (Martínez-Sanz et al., 2018). The produced aerogels and films were stored at 0% RH.

2.5 Density of aerogels

Aerogel densities were determined by measuring the weight and volume of each individual aerogel. The weight of each aerogel was measured by an analytical balance (Precisa Gravimetrics AG SERIES 320XB, Dietikon, Switzerland) and the dimensions were measured by a digital caliper at three different positions.

2.6 Scanning electron microscopy (SEM)

Aerogel samples were coated with a gold-palladium mixture under vacuum and their morphology was studied using a Hitachi microscope (Hitachi S-4800) at an accelerating voltage of 10kV and a working distance of 8-16 mm.

188　**2.7 Water vapour sorption**

189　The water vapour sorption capacity of the aerogels was evaluated by registering the

190　weight gain, using an analytical balance, when placing the samples in a cabinet

191　equilibrated at 25 ºC and 100 % RH. Square samples with a total surface area of 6.25

192　cm^2 were cut from the aerogels and their initial weight was registered. The assays

193　were carried out at least in triplicate.

194

195　**2.8 Water and oil sorption and desorption**

196　Square specimens with a total surface area of 1 cm^2 were cut, weighed and immersed

197　in sealed containers containing 15 mL of distilled water or soybean oil. The samples

198　were periodically taken out of the liquid and weighed after removing the liquid

199　excess. Measurements were taken until the samples were equilibrated and the total

200　weight gain was calculated. After equilibration, the samples were removed from the

201　liquid, placed on top of absorbent paper and left drying at ambient conditions. The

202　weight was registered periodically, until it was constant. The water and oil retention

203　was calculated from the difference between the weight after drying and the initial

204　weight of the samples, before soaking them in the liquids.

205

206　**2.9 Determination of extract composition**

207　The total phenolic compounds in the water-soluble extracts from *A. donax* were

208　estimated by the Folin-Ciocalteu colorimetric assay (Singleton, Orthofer, &

209　Lamuela-Raventós, 1999) and the results were expressed as mg gallic acid (GA)/g

210　extract. The total protein content was measured following the Lowry method (Lowry,

211　Rosebrough, Farr, & Randall, 1951) and the results were expressed as mg bovine

9

212 serum albumin (BSA)/g extract. The total carbohydrate content was determined after

213 sulphuric acid hydrolysis, following the method described in (Martínez-Abad,

214 Giummarella, Lawoko, & Vilaplana, 2018) A detailed description of these protocols

215 can be found elsewhere (Martínez-Sanz et al., 2019). All the determinations were

216 carried out in triplicate.

217

218 **2.10 ABTS Assay**

219 The radical cation scavenging activity of the different lignocellulosic fractions and

220 the water-soluble extracts was determined according to (Re et al., 1999). Briefly,

221 0.192 g of ABTS were dissolved in 50 mL of PBS at pH = 7.4 and mixed with 0.033

222 g of potassium persulfate overnight in the dark to yield the ABTS$^{.+}$ radical cation.

223 Prior to use in the assay, the ABTS$^{.+}$ was diluted with PBS for an initial absorbance

224 of ~0.700 ± 0.02 (1:50 ratio) at 734 nm, at room temperature. Free radical

225 scavenging activity was assessed by mixing 1.0 mL diluted ABTS$^{.+}$ with 10 µL of

226 aqueous suspensions of the samples (5 mg/mL) and monitoring the change in

227 absorbance at 0, 1, 5, 10 min and 24 h. A calibration curve was developed by using

228 6-Hydroxy-2,5,7,8-tetramethylchromane-2-carboxylic acid (Trolox). The antioxidant

229 capacity of test extracts was expressed as mg Trolox equivalents (TE)/g extract. All

230 determinations were carried in triplicate.

231

232 **2.11 β-Carotene-linoleic acid assay**

233 The antioxidant capacity of the extracts and the generated aerogels was evaluated by

234 the β-carotene-linoleic acid assay, according to (Martins et al., 2013), with minor

235 modifications. In brief, 2 mg of β-carotene was dissolved in 10 mL of chloroform. 2

236 mL of this solution were placed on a rotary evaporator and the chloroform was

237 evaporated. Then, 50 µL of linoleic acid and 400 mg of Tween 40 were added and

238 the content of the flask was mixed with stirring. After that, 100 mL of aerated

239 distilled water was transferred to the flask and stirred vigorously. 0.5 mL of ethanolic

240 solutions of the extracts (0.5- 5 mg/mL), BHT (0.5 mg/mL), or 0.5 mL of ethanol as

241 a control were transferred to test tubes and then 5 mL of the β-carotene emulsion

242 were added. For testing the bioactive aerogels, 25 mg of sample was transferred to

243 the tubes and 5 mL of the β-carotene emulsion were added. The samples were

244 incubated in a water bath at 50 °C for 120 min. The absorbance of each sample at

245 470 nm was measured every 15 minutes using a spectrophotometer. The

246 determinations were carried out in duplicate.

247

248 **2.12 *In-vitro* release assays**

249 *In-vitro* release assays were carried out for the bioactive aerogels and films using

250 water and ethanol as the release media. 10 mg of the films and aerogels were soaked

251 in 2 mL of ethanol or water at room temperature. At appropriate time intervals, the

252 concentration of the extract in the release media was estimated by measuring the

253 absorbance of the supernatant at a wavelength of 271 nm using a NanoDrop ND1000

254 spectrophotometer (Thermo Fisher Scientific, USA), until equilibrium was reached.

255 A calibration curve was previously built by recording the whole spectra of the extract

256 diluted in water and ethanol at concentrations ranging from 0.1 mg/mL to 0.5

257 mg/mL. The obtained data were used to determine the total amount of the extract

258 released from the samples at each time point, taking into account that the maximum

259 concentration of extract, if 100% release occurred, was 0.85 mg/mL

260 $(\frac{10\ mg\ aerogel/film}{2\ mL\ H2O/etOH} \cdot \frac{17\ mg\ extract}{100\ mg\ aerogel/film})$. Three independent replicates of each sample

261 were analyzed.

262

263 **2.13 Evaluation of the antioxidant effect of bioactive aerogels on red meat**

264 Bioactive aerogels containing the S-HW extract (F2A + S-HW and F3A + S-HW)

265 and the respective control samples (F2A and F3A) were tested as absorption pads for

266 the preservation of red meat. The aerogels were placed covering the bottom surface

267 of glass Petri dishes (diameter=6 cm) and portions of ca. 12 g of minced beef meat

268 were placed on top of the aerogels. The samples were then sealed with plastic wrap

269 film and stored in the fridge at 4 °C for 10 days. Control samples were prepared by

270 using commercial meat pads and blank samples were prepared by adding the same

271 amount of meat to Petri dishes with no pads.

272

273 **2.13.1 Determination of oxymyoglobin and metmyoglobin**

274 The ability of the aerogels to prevent the colour loss in the red meat after storage was

275 evaluated through the determination of the oxymyoglobin and metmyoglobin content

276 proportions in the raw red meat and in the samples after refrigerated storage for 10

277 days by following the procedure described by Carlez et al. (Carlez, Veciana-Nogues,

278 & Cheftel, 1995). Briefly, two grams of minced meat samples were homogenized

279 with 20 mL of 0.04 mol/L potassium phosphate buffer (pH=6.8). The homogenized

280 samples were kept in an ice bath for 1 h and after that, they were centrifuged at 4200

281 rpm and 10 °C for 30 minutes. The supernatant was then filtered using 0.45 µm pore

282 size filters (Nylon, OlimPeak) and the volume of the filtrate was adjusted to 25 mL

283 with the same phosphate buffer. The absorbance of the supernatant was measured at

12

284   525, 545, 565 and 572 nm in a spectrophotometer. The concentrations of

285   oxymyoglobin and metmyoglobin were calculated using the following equations:

286

287     $\% \, MbO2 = (0.882 \, R_1 - 1.267 \, R_2 - 0.809 \, R_3 + 0.361) \times 100$ (1)

288     $\% \, MetMb = (-2.541 \, R1 + 0.777 \, R_2 + 0.800 \, R_3 + 1.098) \times 100$ (2)

289

290   Where R1, R2, R3 are the absorbance ratios A^{572}/A^{525}, A^{565}/A^{525}, A^{545}/A^{525},

291   respectively.

292   All the determinations were done in triplicate.

293

294   **2.13.2 Measurement of lipid oxidation**

295   The degree of lipid oxidation in the red meat samples after 10 days of storage was

296   also measured by following the 2-thiobarbituric acid (TBA) distillation method

297   (Tang, Sheehan, Buckley, Morrissey, & Kerry, 2001). 10.0 g of meat were

298   homogenised with 30 mL of water. The sample was then transferred to a distillation

299   flask with 65 mL of water and the pH was adjusted to 1.5 with HCl 4N. Ethanolic

300   propyl gallate (10%, 1mL), 10% EDTA (disodium salt, 1 mL), and a drop of

301   antifoaming agent were added. The flask was connected to a Soxhlet apparatus and

302   the mixture was boiled until 50 mL of distillate was collected. In a screw capped test

303   tube, 5 mL of the distillate was reacted with 5 mL of TBA reagent (0.02 M TBA in

304   90% acetic acid) in a boiling water bath for 35 min. A control made up of 5 mL

305   distilled water and 5 mL of TBA reagent was also boiled for 35 min. The tubes were

306   cooled to room temperature and the absorbance was measured at 535 nm in a

307   spectrophotometer. The TBA reactive substances (TBARS) were calculated by

308 multiplying the absorbance readings by a factor of 7.8 and expressed as mg

309 malondialdehyde (MDA)/Kg meat. The inhibition of lipid oxidation was calculated

310 as follows:

311

312 $Inhibition\ (\%) = \frac{(TBARS_{Blank} - TBARS_{Day\ 0}) - (TBARS_{Pad} - TBARS_{Day\ 0})}{(TBARS_{Blank} - TBARS_{Day\ 0})} \times 100$ (3)

313

314 Where $TBARS_{Day\ 0}$ refers to the TBARS in the raw minced meat and $TBARS_{Blank}$

315 and $TBARS_{Pad}$ correspond to the TBARS in the meat samples after 10 days of

316 refrigerated storage (blank sample and samples with the commercial or the cellulosic

317 aerogel pads, respectively). These determinations were carried out in triplicate.

318

319 **2.14 Statistics**

320 All data have been represented as the average ± standard deviation. Different letters

321 show significant differences both in tables and graphs (p≤0.05). Analysis of variance

322 (ANOVA) followed by a Tukey-test were used when comparing more than two data

323 sets.

324

325 **3. Results**

326 **3. 1 Characterization of cellulosic aerogels**

327 Aquatic biomass from the invasive species *A. donax* was valorized for the extraction

328 of different holocellulosic fractions, as described in a previous work (Martínez-Sanz

329 et al., 2018). These fractions were previously used to produce films by a simple

330 vacuum filtration method and their properties were seen to be significantly different

14

331   depending on the source (stems vs. leaves) and the extraction protocol (Martínez-

332   Sanz et al., 2018). In this work, the extracted fractions were dispersed in water and

333   subsequently freeze-dried to generate aerogel structures. As shown in Figure 1A, the

334   obtained aerogels consisted of whitish sponge-like materials, with a soft consistency

335   but good mechanical integrity (see also Figure S1). The aerogels obtained from the

336   leaf fractions (F2L and F3L) were more heterogeneous than the homologous aerogels

337   obtained from the stem fractions (F2A and F3A). In particular, the F2L aerogel

338   presented a very soft consistency and poor integrity. It was also observed that the

339   more purified cellulose aerogels presented a whiter coloration than the less purified

340   ones. Specifically, the presence of hemicelluloses and lipids in the F2A and F2L

341   aerogels conferred them a brownish hue.

342

343   The morphology of the aerogels was characterized by SEM and representative

344   images are shown in Figure 1B. As observed, in general the aerogels presented an

345   open porous network structure. It appears that those aerogels composed of fractions

346   where the hemicelluloses had been removed (i.e. F3, F3A and F3L) presented a more

347   compacted structure with less pores than their analogous aerogels containing

348   hemicelluloses. Comparing the aerogels obtained from fractions extracted with (F2

349   and F3) and without (F2A and F3A) the Soxhlet treatment, it seems that the presence

350   of lipidic impurities also promoted the formation of slightly more porous structures.

351   Moreover, it should be noted that the aerogels obtained from leaf biomass fractions

352   (F2L and F3L) presented a more heterogeneous structure, especially F2L, where

353   large fibrillar aggregates were also detected. This can be attributed to the presence of

354   higher amounts of impurities such as minerals and proteins in the leaf biomass

355 (Martínez-Sanz et al., 2018), suggesting that stem fractions are more suitable for the

356 production of aerogels. Thus, it seems that a higher degree of cellulose purity led to

357 the formation of more homogenous and continuous structures, while the presence of

358 other components resulted in the formation of more porous structures.

359
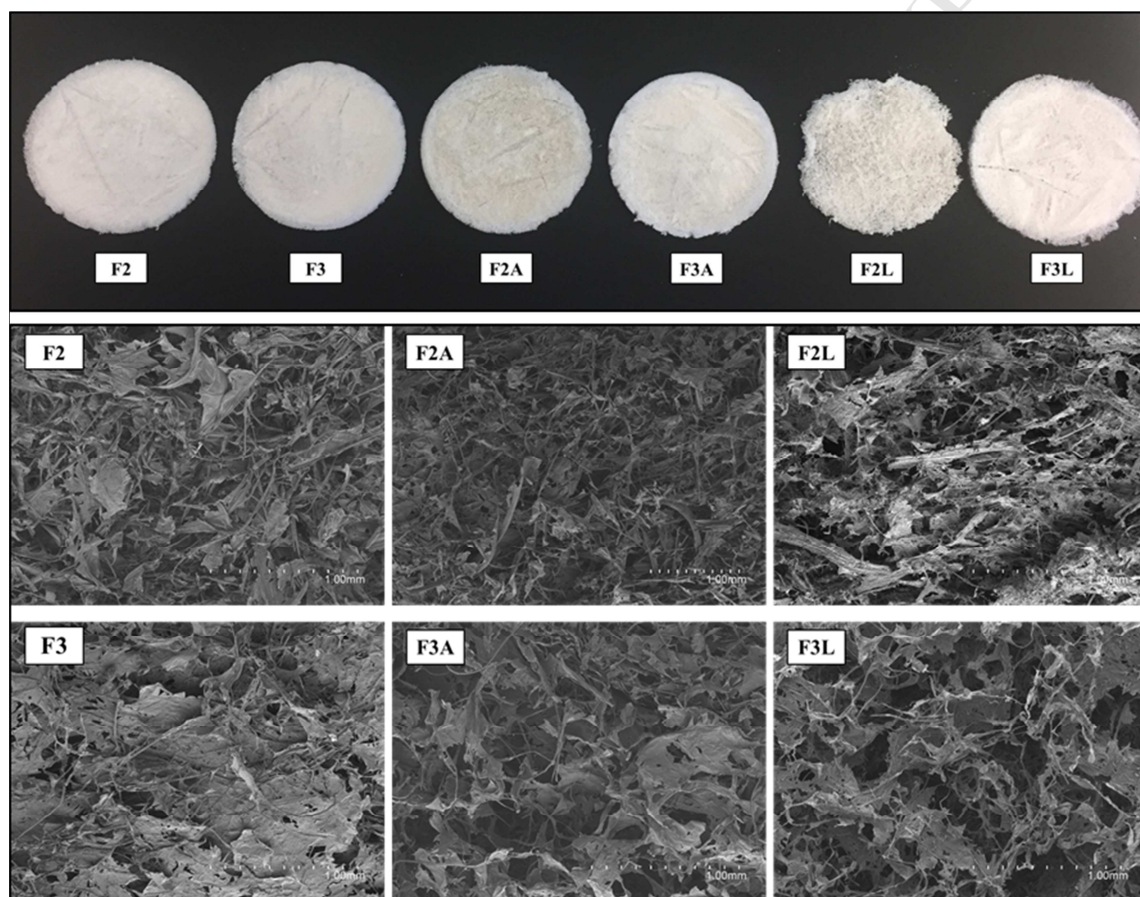
360

361 **Figure 1.** (A) Visual appearance and (B) SEM micrographs of the surface from the

362 *A. donax* cellulosic aerogels.

363

364 The density of the aerogels was estimated and the results are summarized in Table 1.

365 Although the differences were not statistically significant, the more purified cellulose

366 aerogels seemed to present greater density values than the aerogels containing

367 hemicelluloses, supporting the porosity differences observed by SEM. The F2L

368   aerogel presented an anomalously high density, which may be the result of its more

369   heterogeneous structure. On the other hand, the F2A aerogel was the most

370   lightweight material, corresponding with its more open porous structure (cf. Figure

371   1A). The densities of most aerogels were significantly lower than those previously

372   reported for aerogels prepared by solvent exchange and supercritical CO_2 drying of

373   cellulose solutions in NMMO (ca. 50 mg/cm^3) (Innerlohinger et al., 2006) and

374   cellulose nanowhiskers aqueous suspensions (78 mg/cm^3) (Heath & Thielemans,

375   2010), having the same cellulose concentration used in this work (i.e. 0.5 wt.-%) and

376   similar to aerogels produced by supercritical CO_2 drying of regenerated tunicate

377   cellulose (10 mg/cm^3) (Cai, Kimura, Wada, Kuga, & Zhang, 2008). In contrast,

378   lower density values (down to 6-8 mg/cm^3) have been reported for optimized

379   aerogels produced by means of freeze-drying of aqueous suspensions of rice straw

380   cellulose nanofibrils produced by coupled TEMPO-oxidation and mechanical

381   blending (Jiang & Hsieh, 2014a, 2014b).

382

383   **Table 1.** Density and water vapour sorption of the cellulosic aerogels.

	Density (mg/cm^3)	Water vapour sorption (g/g aerogel)
F2	12.84 ± 0.0029^{ab}	0.91 ± 0.02^b
F3	13.77 ± 0.0053^{ab}	0.39 ± 0.04^c
F2A	10.21 ± 0.0010^b	0.83 ± 0.02^b
F3A	14.39 ± 0.0004^{ab}	0.41 ± 0.02^c
F2L	25.55 ± 0.0057^a	1.09 ± 0.01^a
F3L	12.55 ± 0.0008^{ab}	0.52 ± 0.05^c

384   Values with different letters are significantly different (p $\leq$0.05).

385

386   The highly porous structure of cellulose aerogels offers a great advantage for the

387   development of superabsorbent materials and/or matrices for the selective release of

388   bioactive components in different media. The differences in composition and

389   structure of the developed aerogels are expected to affect their behaviour when

390   exposed to different media, which will ultimately determine their suitability to be

391   used as template for the sorption and/or release of bioactive extracts. The water

392   vapour sorption capacity of the aerogels was evaluated gravimetrically by exposing

393   the samples to 100% RH conditions and the results are summarized in Table 1. As

394   observed, the presence of hemicelluloses in the aerogels clearly had a significant

395   impact, leading to increased water sorption capacity. This might be attributed to (i)

396   the more hydrophilic character of hemicelluloses, provided by the greater amount of

397   free hydroxyl groups in their structure and to their amorphous structure, as opposed

398   to cellulose, which presents a more crystalline structure, with greater degree of self-

399   association (Benito-González et al., 2018) and (ii) the more porous aerogel structure

400   induced by the presence of hemicelluloses. The same trend has been previously

401   reported for films produced from the cellulosic fractions extracted from *A. donax*,

402   although the absolute water uptake values obtained for the films (0.06-0.1 g/g film

403   for the films containing hemicelluloses and 0.02-0.05 g/g film for the purified

404   cellulose films) (Martínez-Sanz et al., 2018) were significantly lower than those

405   estimated for the aerogels, hence evidencing the great impact of the porosity on the

406   sorption capacity. It is also worth noting that the presence of minor amounts of

407   lipidic impurities in the aerogels obtained from fractions without the Soxhlet

408   treatment did not have an impact on the water vapour sorption.

409

18

410   Further to the behaviour of the aerogels when exposed to high relative humidity,

411   which could take place, for instance, upon storage of foodstuffs at ambient

412   conditions, their capacity to absorb and retain hydrophilic and hydrophobic media

413   was also evaluated through immersion in water and soybean oil and subsequent

414   drying at ambient conditions. All the aerogels were able to maintain their integrity,

415   even after soaking them for 24h in both media. Figure S2 shows the

416   sorption/desorption kinetics and Figure 2 displays the sorption equilibrium values

417   (after immersion in the liquid media and after subsequent drying). As observed, both

418   water and oil were quickly absorbed into the aerogels, reaching equilibrium values

419   approximately after 24h. When drying the samples at ambient conditions, water was

420   quickly released from the aerogels, producing a steep weight decrease within the first

421   30 min and reaching the equilibrium after ca. 2 h. In contrast, the drying process took

422   place more slowly in the case of oil, which was expected due to its higher viscosity

423   (ca. 0.041 Pa·s at 20ºC (Diamante & Lan, 2014) versus 0.001 Pa·s for water) and

424   evaporation temperature. A sharper weight loss occurred during the first 3 h,

425   reaching the equilibrium after ca. 7-8 h. A significant amount of both water and oil

426   was released from the aerogels upon drying and, thus, the retention values were

427   much lower than the sorption capacities, indicating that a significant amount of the

428   absorbed liquids was not strongly interacting with the aerogel matrix materials. It

429   should be noted that the lowest water and oil sorption capacity values corresponded

430   to the F2L aerogel, which can be related to its heterogeneous structure.

431

432   For the water sorption/desorption process, the aerogels containing hemicelluloses

433   showed a faster sorption/desorption kinetics than their more purified counterparts,

19

434   which can be attributed to their more porous structure. Furthermore, the water

435   sorption equilibrium values were greater for the hemicellulose-containing aerogels.

436   This can be ascribed to the greater compatibility of the more hydrophilic

437   hemicelluloses with water, as compared with the cellulose hydrogels, where less

438   amount of free hydroxyl groups may be available on the surface of the pore walls due

439   to strong self-association. In fact, Chen et al. (2011) reported that aerogels with

440   higher cellulose contents lead to the formation of stronger hydrogen bonding

441   networks, resulting in a decreased water uptake. It should also be noted that the

442   aerogels obtained from fractions without the Soxhlet treatment, containing

443   hydrophobic lipidic impurities, showed lower water and oil sorption capacities than

444   their purified counterparts. These results suggest that although the water

445   sorption/desorption process was mostly a physical phenomenon, the affinity and

446   interactions established between the components in the aerogels and the water played

447   also an important role. This can be explained by the existence of two different

448   adsorbed water domains, as previously reported for silica aerogels: (i) one fraction of

449   bound water interacting with the aerogel components through hydrogen bonding and

450   (ii) one fraction of bulk water which is physically adsorbed within the aerogel pores

451   (Da Silva, Donoso, & Aegerter, 1992).

452

453   In the case of the soybean oil, the opposite trend was observed for the sorption

454   process, i.e. the more purified cellulose-based aerogels presented faster kinetics and

455   reached greater oil sorption equilibrium values. In particular, the purest cellulose

456   aerogel, i.e. F3, presented the greatest oil sorption capacity. This seems to confirm

457   the more hydrophobic behaviour of the cellulose-based aerogels due to the strong

458   cellulose self-association, facilitating the oil sorption process. However, although the

459   more purified aerogels seemed to show a faster oil desorption process, no significant

460   differences were encountered between the oil retention values for all the samples.

461   The soybean oil retention values were greater than those for water for all the

462   samples, which is explained by the stronger effect of capillary forces in the case of

463   the more viscous oil, a fraction of which remained adhered to the pore walls and

464   trapped within the macropores (Hu, Zhao, Gogotsi, & Qiu, 2014). The same effect

465   has been previously observed for oils with different viscosities (Feng, Nguyen, Fan,

466   & Duong, 2015; Nguyen, et al., 2013).

467

468   The values previously reported in the literature for the sorption of liquids of

469   cellulose-based aerogels evidence the excellent capacity of the *A. donax* aerogels to

470   absorb liquid media, without the need of any physical or chemical modification. A

471   lower water sorption capacity of 19.8 g water/g aerogel has been previously reported

472   for aerogels from native recycled cellulose (Nguyen et al., 2014). Only modified

473   cellulose aerogels have been shown to present greater water sorption capacities. For

474   instance, water sorption values of 104-210 g water/g aerogel have been reported for

475   aerogels from TEMPO-oxidized and defibrillated cellulose nanofibers (Jiang &

476   Hsieh, 2014a, 2014b). It should be noted that these aerogels possessed a less dense

477   structure than the ones developed in this work, confirming the relevance of the

478   porosity for the liquid sorption capacity of the aerogels. Salam et al. (2011) obtained

479   hemicellulose aerogels incorporating carboxylic groups from a reaction with citric

480   acid followed by cross-linking with chitosan, increasing the water sorption capacity

481   up to 100 g water/g sample. With regards to the oil sorption capacity, lower values of

482   18-20 g crude oil/g aerogel were reported for methyltrimethoxysilane-coated

483   cellulose aerogels (Nguyen et al., 2013) and a similar value of 62.6 g motor oil/g

484   aerogel was obtained for cross-linked and hydrophobized 0.5 wt.-% cellulose

485   aerogels (measured at 25 ℃) (Feng, et al., 2015). The authors reported a maximum

486   sorption capacity of 95 g motor oil/g aerogel, which could be achieved by lowering

487   the cellulose concentration down to 0.25 wt.-% and producing less dense and more

488   porous structures. Lower sorption capacities for different oils and organic solvents

489   have also been reported for nanocellulose aerogels chemically modified to increase

490   their hydrophobicity (Mulyadi, Zhang, & Deng, 2016; Phanthong et al., 2018).

491

492

493
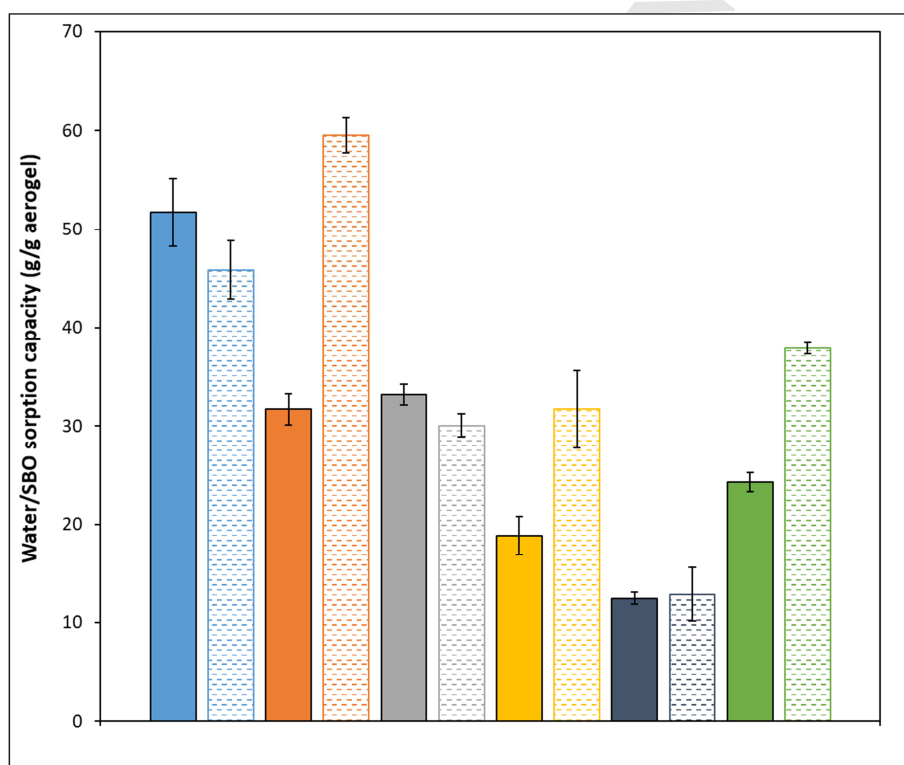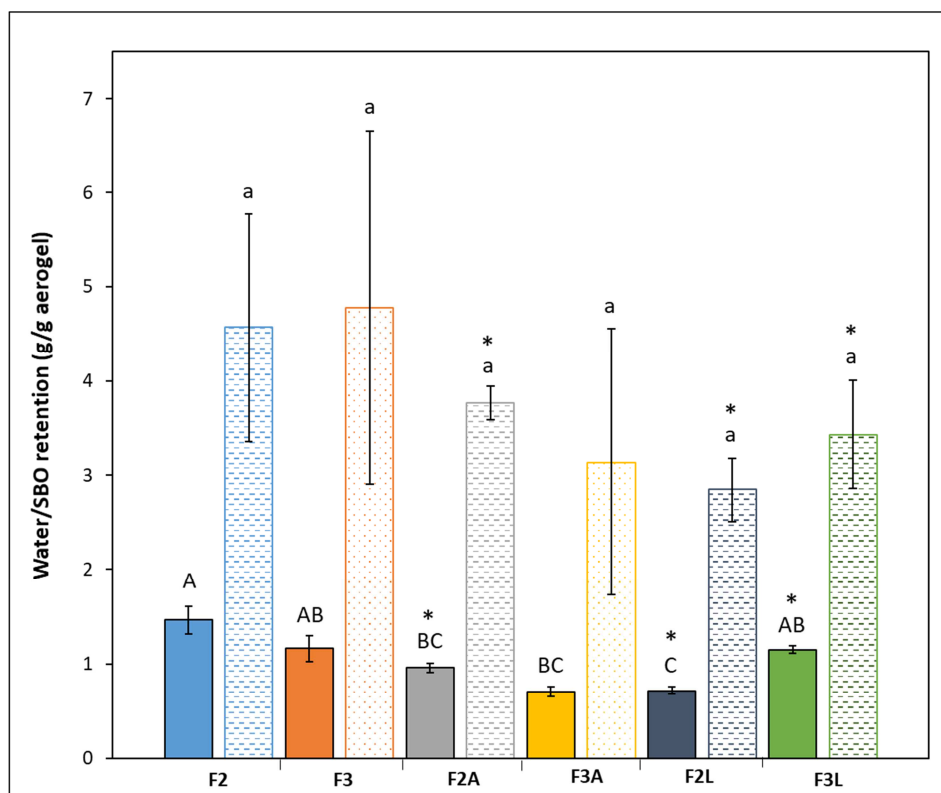
Figure 2. (A) Water and soybean oil sorption capacity and (B) water/oil retention capacity of the *A. donax* cellulosic aerogels after drying at ambient conditions. Solid bars represent the water sorption/retention values and patterned bars represent the soybean oil sorption/retention values. Bars with different letters are significantly different (p ≤0.05). * indicates significant differences (p≤0.05) for the same sample when soaked in water and oil.

The overall objective of this work was to generate bioactive aerogel structures by utilizing the waste biomass from *A. donax*. Since some of the components remaining in the less purified extracts, such as polyphenols, proteins and lipids may present antioxidant properties, the different cellulosic fractions, prior to the preparation of the aerogels, were characterized by means of the ABTS assay. From the results compiled in Table S1, it is clear that (i) the stem fractions presented higher

23

508 antioxidant capacity than the leaf fractions and (ii) the components remaining in the

509 less purified fractions conferred them greater antioxidant capacity. These results

510 show the potential of the less purified aerogels to be used as bioactive food

511 packaging structures.

512

513 **3.2 Production and characterization of water-soluble extracts from *A. donax***

514 Aquatic plants and algae are known to contain bioactive components such as

515 polyphenols and sulphated polysaccharides that possess bioactive functionalities.

516 Thus, the biomass from *A. donax* (stems and leaves) was also utilized to produce

517 water-soluble extracts and their composition and antioxidant capacity were

518 evaluated. To generate the extracts, two different protocols based on hot-water and

519 ultrasound treatments were explored. The composition of the four different extracts

520 was determined and the results are compiled in Table 2. As observed from this table,

521 while polysaccharides were the main component in the stem extracts, similar

522 amounts of proteins and polysaccharides were detected in the leaf extracts. It should

523 be noted that, in general, the hot water treatment promoted the extraction of

524 polysaccharides and polyphenols.

525

526 The antioxidant capacity the extracts was measured by using the ABTS and β-

527 carotene bleaching assays. The first method is based on the scavenging capacity of

528 the tested extract against the ABTS radical, converting it into a colourless product.

529 On the other hand, the second protocol quantifies the ability of the extract to prevent

530 the β-carotene degradation when subjected to high temperatures. The results listed in

531 Table 2 evidence that the S-HW extract presented the highest antioxidant capacity

24

532   according to the ABTS assay, which can be related to the higher content of

533   polysaccharides and polyphenols in this extract. To the best of our knowledge, no

534   previous data on the antioxidant capacity of aqueous *A. donax* extracts are available.

535   In general, organic solvents are preferred to produce plant extracts with antioxidant

536   capacity, since bioactive compounds such as non-glycosilated flavonoids,

537   phospholipids, carotenoids and chlorophyll analogues, are known to be more soluble

538   in these solvents. However, other bioactive compounds such as sulphated

539   polysaccharides and glycosylated polyphenols present a more hydrophilic character.

540   In fact, lower antioxidant capacity values of ca. 70 µmol TE/g extract have been

541   reported for the acetone extracts from *A. donax* leaves (Piluzza & Bullitta, 2011),

542   which can be directly related to their lower polyphenol content (ca. 21 mg GA/g

543   extract) (Piluzza & Bullitta, 2011). The aqueous *A. donax* extracts presented greater

544   phenolic contents than those previously reported in the literature for the methanolic

545   extracts from a range of aquatic plants (1.6-21.6 mg GA/g extract) (Dellai, Laajili,

546   Morvan, Robert, & Bouraoui, 2013; Kannan, Arumugam, Thangaradjou, &

547   Anantharaman, 2013). Thus, the results seem to point out that *A. donax,* in particular

548   the stem fraction, is rich in polysaccharides and polyphenols which confer the

549   aqueous extracts a relatively high antioxidant capacity.

550

551   With regards to the capacity of the extracts to inhibit the β-carotene bleaching,

552   Figure S2 shows the effect of the extracts when tested at three different

553   concentrations, while the values compiled in Table 2 correspond to the highest

554   concentration of 5 mg/mL. From Figure S3, increasing the extract concentration

555   seemed to slightly improve the inhibition capacity, although the effect was not

556 significant due to the large standard deviation values. It should be highlighted that

557 the extracts presented similar antioxidant activities to that of a commercial synthetic

558 antioxidant such as BHT. No significant differences amongst the extracts were found

559 at a concentration of 5 mg/mL, although the S-HW extract showed the highest

560 percentage of inhibition. To the best of our knowledge, the capacity of *A. donax*

561 extracts to inhibit the β-carotene bleaching has not been reported in the literature,

562 although data for other plant extracts can be found in the literature. For instance, the

563 aqueous extract from *Tossa jute* leaves has been reported to present ca. 70.8%

564 inhibition when tested at 0.5 mg/mL (Ben Yakoub et al., 2018) and the ethanolic

565 extracts from *Osmundaria obtusiloba* and *Pterocladiella capillacea* have shown 90%

566 and 45% inhibition, respectively, when tested at a concentration of 1 mg/mL (De

567 Alencar et al., 2016). Thus, although no reference values could be found in the

568 literature for a fair comparison, the β-carotene bleaching results, together with the

569 ABTS assay, seem to evidence the high antioxidant capacity of the aqueous *A. donax*

570 extracts.

571

572 **Table 2**. Composition and antioxidant activity of *A. donax* water-soluble extracts.

	Polysaccharides (mg/g sample)	Proteins (mg BSA/g extract)	Polyphenols (mg GA/g sample)	TEAC (µmol TE/g sample) [*]	β-Carotene bleaching inhibition (%) [†]
S-HW	432.3 ± 84.6^a	150.0 ± 2.1^a	52.3 ± 0.9^a	143.7 ± 17.2^a	93.3 ± 0.7^a
L-HW	170.1 ± 51.2^b	143.7 ± 0.7^a	43.7 ± 3.4^{ab}	$86. \pm 7.2^b$	86.9 ± 14.9^a
S-US	224.4 ± 16.4^b	149.3 ± 11.0^a	35.4 ± 5.4^b	97.1 ± 11.9^b	84.76 ± 12.32^a
L-US	117.1 ± 28.8^b	148.5 ± 8.5^a	35.2 ± 1.0^b	79.6 ± 5.3^b	60.80 ± 16.05^a

573 Values with different letters are significantly different (p ≤0.05).

574 [*] TEAC values were calculated after 10 minutes.

575 [†] Calculated for the extracts at a concentration of 5 mg/mL.

576

577 **3.3 Production of bioactive aerogels**

578 Highly porous, superabsorbent aerogels and bioactive extracts from *A. donax*

579 biomass were generated by green processes. Subsequently, these two components

580 were combined to develop bioactive aerogels for food packaging applications. The

581 F2A and F3A aerogels were selected as the matrices for several reasons: (i) these

582 fractions were produced by a more cost-effective and greener process in which the

583 use of organic solvents was avoided, (ii) they showed greater inherent antioxidant

584 capacity and (iii) the produced aerogels showed excellent water and oil sorption

585 capacities (although lower than the more purified F2 and F3 aerogels) and, thus, they

586 were good candidates for the incorporation and release of bioactive extracts. The S-

587 HW extract was selected due to its higher antioxidant capacity and it was

588 incorporated into the F2A and F3A aerogels at a concentration of 17 wt.-%, which

589 was the maximum concentration allowing to preserve the integrity of the aerogels.

590

591 In order to evaluate the release of the bioactive extract from the F2A and F3A

592 aerogels when exposed to different liquid media, *in-vitro* release studies were carried

593 out in ethanol and water. Additionally, to assess the impact of the material porosity

594 in the release behaviour, F2A and F3A films, presenting a much more compact

595 structure (Martínez-Sanz et al., 2018), were also prepared by incorporating the same

596 amount of extract. The results from the release studies, shown in Figure 3, indicate

597 that, in general, the less purified F2A fraction provided greater extract release than

598 the F3A fraction, both in films and aerogels. When water was selected as the release

599 medium, a steeper release took place in the aerogels during the first 25 minutes, but

27

600 after that both aerogels and films showed a much slower release, reaching the

601 equilibrium after ca. 3-4 h (ca. 100% release for the F2A aerogel, 84% for the F3A

602 aerogel, 86% for the F2A film and 56% for the F3A film). The greater release values

603 in the aerogels may be directly linked to their morphology, i.e. their porous structure

604 facilitated the diffusion of water inwards and outwards the aerogel structure and as a

605 consequence, promoted the quick release of the hydrophilic extract. In contrast, the

606 compact structure of the films hindered the accessibility of water, releasing mostly

607 the extract present on the surface of the films during the beginning of the experiment.

608 Furthermore, stronger matrix-extract interactions seem to have been developed in the

609 case of the films, hence leading to lower amounts of extract released after reaching

610 the equilibrium. Moreover, in agreement with the water swelling experiments (cf.

611 Figures 2A and 2B), the F2A aerogel seemed to promote water diffusion to a greater

612 extent, thus increasing the amount of hydrophilic extract released to the liquid

613 medium. Bacterial cellulose aerogels loaded with L-ascorbic acid and dexpanthenol,

614 prepared by antisolvent precipitation with supercritical CO_2, showed similar release

615 profiles, achieving 100% release of the bioactives after ca. 2-3 h and the authors

616 claimed that the release process was purely diffusion driven (Haimer et al., 2010).

617 On the other hand, Valo et al., 2013 observed that the release of a drug incorporated

618 into nanocellulose aerogels obtained from different sources was not only dependent

619 on the structure but was also strongly affected by the interactions between the drug

620 nanoparticles and the cellulose matrix, reaching equilibrium release values of ca. 40-

621 60% for those cellulose aerogels where stronger interactions with the drug were

622 established.

623

624 The use of a less polar solvent such as ethanol reduced the amount of released extract

625 in the case of the aerogels. Interestingly, in that case very similar or even lower

626 release values were obtained for the aerogels (ca. 62% for the F3A aerogel and 77%

627 for the F2A aerogel) as compared with the films (ca. 60% for the F3A film and 99%

628 for the F2A film). This might be due to a reduced diffusion of ethanol through the

629 aerogel pores due to the lower affinity of this solvent with the cellulosic components.

630 These results seem to indicate that while the release of the extract took place mostly

631 at the surface level in the case of the films, a liquid medium diffusion-induced

632 release mechanism took place in the case of the aerogels. Thus, the aerogels offer a

633 clear advantage for their application as bioactive food packaging structures, since

634 they are expected to release large amounts of extract when placed in contact with

635 high moisture content foodstuffs.

636

637
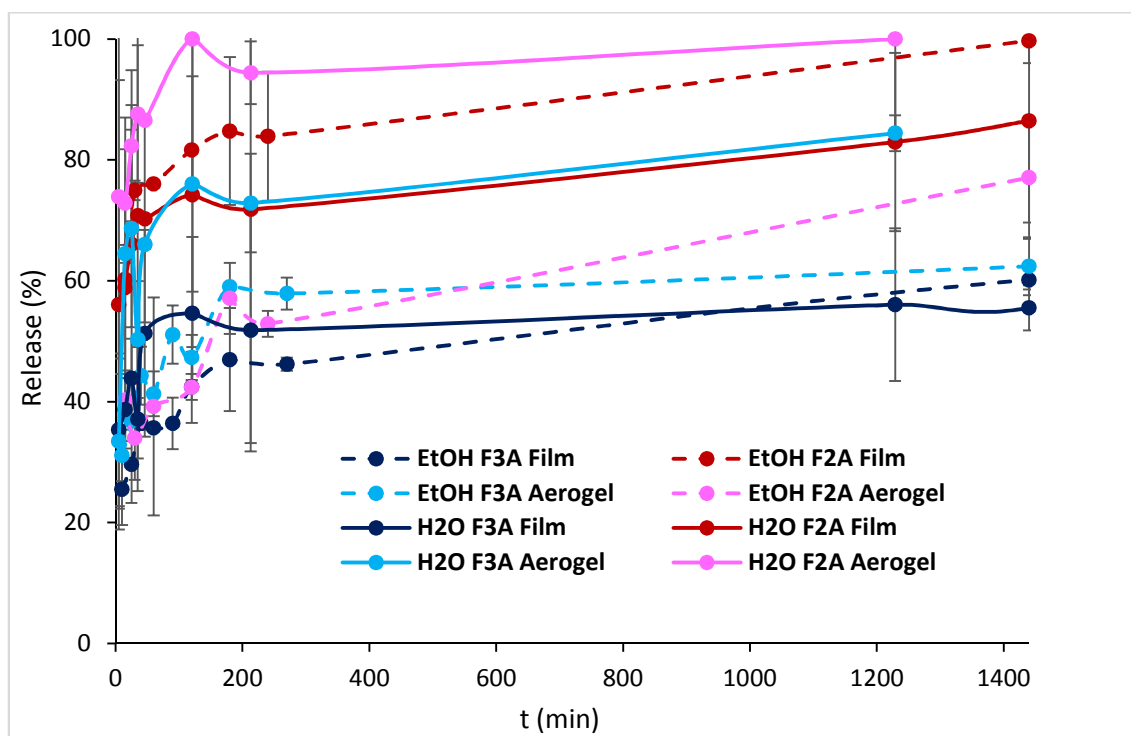
Figure 3. Release profiles of S-HW extract from *A. donax* aerogels and films in ethanol and water.

640

641   The high release of the bioactive S-HW extract when the aerogels were subjected to

642   high moisture conditions, together with the inherent antioxidant effect of the F2A

643   and F3A fractions, were expected to confer the hybrid aerogels antioxidant capacity.

644   To confirm this and to compare the performance of aerogels and films, the β-

645   carotene bleaching assay was carried out by soaking film and aerogel samples in the

646   β-carotene emulsion. Since the cellulosic fractions were previously observed to

647   present antioxidant potential, the pure films and aerogels with no added extract were

648   firstly tested. As observed in Table 3, the aerogels, in particular the F2A aerogel,

649   were able to reduce the degradation of β-carotene, while the films did not show a

650   significant effect. This confirms that (i) the F2A fraction presented greater

651 antioxidant capacity due to the presence of impurities like phenolic compounds and

652 (ii) the release of bioactive components into aqueous media is favoured in the porous

653 aerogels as compared to the compact-structured films. The β-carotene bleaching

654 inhibition of the hybrid aerogels and films, containing the S-HW extract was then

655 evaluated and the difference between the obtained inhibition values and those

656 corresponding to the pure aerogels and films was calculated to evaluate the effect of

657 the incorporated extract. On the other hand, the inhibition of the pure extract at the

658 same concentration present in the films and aerogels (i.e. 0.84 mg/mL) was estimated

659 as 58.8 ± 0.9 %. The results, gathered in Table 3, show that the hybrid F2A aerogel

660 provided the greatest inhibition capacity. Interestingly, no significant differences

661 were found between the analogous aerogels and films when removing the

662 contribution from the matrices (see third column in Table 2), suggesting that the

663 extract was released to the same extent in both types of structures when heating up to

664 50ºC for 120 min. Furthermore, and in agreement with the *in-vitro* release

665 experiments, the results indicate that stronger matrix-extract interactions must have

666 been established in the case of the F3A aerogel/film, limiting the release. Overall, the

667 hybrid F2A aerogel presented the highest inhibition percentage, thus being the most

668 promising material for the development of antioxidant food packaging structures.

669

670 **Table 3.** Antioxidant capacity of *A. donax* aerogels and films, measured from the β-

671 carotene bleaching assay.

	β-Carotene bleaching inhibition (%)		
	Pure Aerogel/Film	Aerogel/Film + S-HW	(Aerogel/Film + S-HW) – Aerogel/Film
Aerogel F2A	32.8 ± 8.8^{a}	90.1 ± 2.8^{a}	57.3 ± 2.9^{a}
Aerogel F3A	19.3 ± 0.7^{ab}	57.7 ± 0.06^{b}	38.4 ± 0.1^{b}

Film F2A	5.6 ± 3.2^b	58.9 ± 4.4^b	53.3 ± 4.4^{ab}
Film F3A	5.7 ± 1.5^b	42.5 ± 6.1^b	36.8 ± 6.1^b

672 Values with different letters are significantly different ($p \leq 0.05$).

673
674
675 **3.4 Evaluation of the antioxidant effect of bioactive aerogels on red meat**
676
677 As a final proof of concept, the hybrid and the pure cellulosic aerogels were tested as

678 absorption pads to inhibit lipid oxidation and colour loss during storage of minced

679 red meat. Meat discoloration is attributed to the process of oxymyoglobin oxidation,

680 giving rise to the formation of metmyoglobin. The proportion of these two

681 myoglobin forms was determined in the raw minced meat and in the samples after

682 storage for 10 days. The visual appearance of representative meat samples after

683 storage is shown in Figure 4A and the estimated myoglobin contents are shown in

684 Figure 4B. It is observed that at day 0 (i.e. fresh meat) the oxymyoglobin content was

685 higher than metmyoglobin, as expected. After storage, a colour loss, indicated by the

686 lower oxymyoglobin content and the higher metmyoglobin content, took place in all

687 the samples. Interestingly, and as supported by Figure 1A, the samples stored with

688 aerogel pads presented higher oxymyoglobin and lower metmyoglobin content than

689 the control sample prepared using commercial pads, highlighting the potential of

690 these materials to limit the oxidation processes giving rise to meat discoloration upon

691 storage. In particular, the F2A+S-HW aerogel showed the strongest effect, which

692 may be attributed to the antioxidant capacity of its components (both the extract and

693 the F2A fraction). To the best of our knowledge, no previous works have reported on

694 the utilization of aerogel structures or cellulose-based materials as antioxidant food

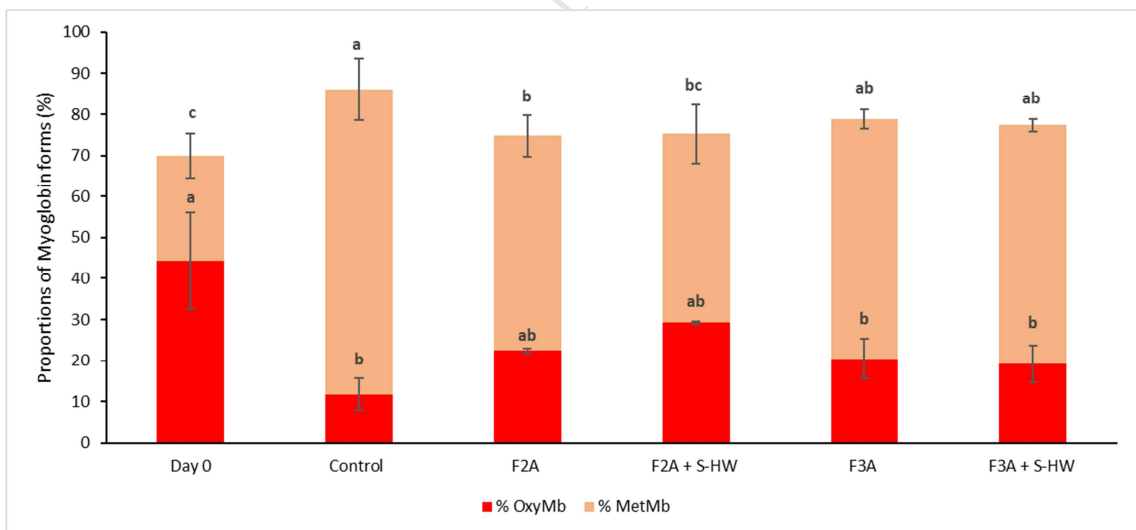695 packaging structures. As a reference, 60% of metmyoglobin was detected in foal

696 meat after storage for 10 days in modified atmosphere using bioactive films

697 containing oregano extract (Lorenzo et al., 2014), which is higher than the value

698 estimated for the meat stored in contact with the F2A+S-HW aerogel (ca. 46%

699 metmyoglobin).

700
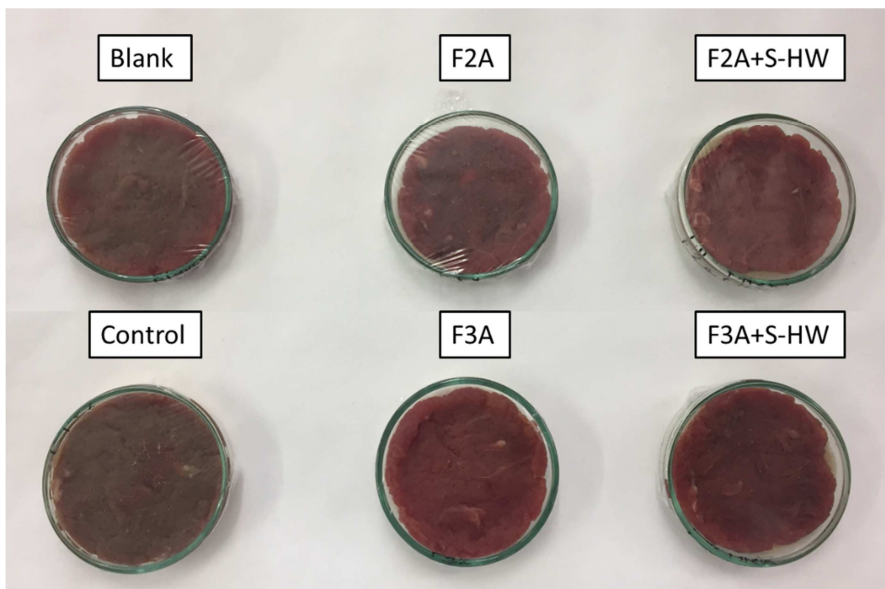
701

702

703 **Figure 4.** (A) Visual appearance of the meat samples after storage for 10 days. (B)

704 Proportions of oxymyoglobin (%OxyMb) and metmyoglobin (%MetMb) in the raw

705 minced red meat (day 0) and in the meat after 10 days of storage. Bars with different

706 letters are significantly different (p ≤0.05).

707

708 The ability of the developed aerogels to prevent lipid oxidation in red meat was also

709 evaluated by calculating the TBARS content in the raw minced meat and in the

710 samples after storage and estimating the percentage of lipid oxidation inhibition with

711 regards to a blank sample (i.e. meat stored without any pad). Although, as seen from

712 the results summarized in Table 4, due to the large standard deviation values arising

713 from the large inherent variability of the meat samples, no significant differences

714 were found between samples, the meat stored in contact with the F2A+S-HW aerogel

715 showed the lowest TBARS content and the highest lipid oxidation inhibition. To the

716 best of our knowledge no previous works have reported on the potential of highly

717 porous cellulose-based aerogels as bioactive food packaging structures. The most

718 typical approach reported in the literature to prevent lipid oxidation in meat consists

719 on the utilization of natural extracts. For instance, active packaging films containing

720 2% of oregano essential oil or 1% of green tea extract were utilized to store foal

721 steaks, although no significant effect in the TBARS content was detected after 10

722 days of storage (Lorenzo et al., 2014). In another work, meat steaks were packaged

723 in polystyrene trays and sprayed with oregano extract. The addition of 0.5% of

724 oregano extract showed a high inhibitory effect on lipid oxidation, reaching a

725 maximum value of 2 mg malonaldehyde/Kg meat after 28 days of storage (Camo et

726 al., 2011). These results, together with the results from the meat colour evaluation

727 and the antioxidant capacity of the aerogels, evidence the antioxidant potential of the

728 F2A+S-HW aerogel, which could be used as bioactive pads in high moisture fresh

729 packaged foods such as red meat.

730

731 **Table 4.** 2-thiobarbituric acid reactive substances (TBARS) and estimated lipid

732 oxidation inhibition in the raw minced red meat (day 0) and in the meat after 10 days

733 of storage.

	TBARS (mg malonaldehyde/ Kg meat)	Lipid oxidation Inhibition (%)
Day 0	0.53 ± 0.15^b	---
Control	6.37 ± 1.68^a	2.2
F2A	4.36 ± 1.25^{ab}	35.9
F2A+S-HW	4.04 ± 2.34^{ab}	41.3
F3A	4.84 ± 0.89^{ab}	27.9
F3A+S-HW	$4.57. \pm 1.50^{ab}$	32.3

734 Values with different letters are significantly different ($p \leq 0.05$).

735

736 **4. Conclusions**

737 Highly porous bio-based bioactive aerogels have been produced by valorizing the

738 lignocellulosic waste biomass from *A. donax* biomass. Cellulosic aerogels were

739 produced by a simple freeze-drying method from aqueous suspensions of the

740 fractions extracted from *A. donax* stems and leaves. All the developed aerogels

741 presented an excellent water and oil sorption capacity, comparable to those

742 previously reported for chemically modified nanocellulose aerogels. The presence of

743 hemicelluloses in the F2 and F2A aerogels conferred them a less dense, more porous

744 structure, as well as a more hydrophilic character, promoting water sorption through

745 diffusion and water-hemicelluloses interactions.

746

747 Additionally, aqueous extracts with high antioxidant capacities were generated by

748 subjecting the *A. donax* biomass to simple heating and ultrasound methods. The

749 higher polysaccharide and polyphenol content in the stems extract generated by

35

750 heating (S-HW) conferred it the highest antioxidant capacity. This extract was

751 incorporated into the F2A and F3A aerogels, which were selected due to their good

752 water sorption capacity, their inherent antioxidant potential and their greater

753 suitability from an economical and environmental perspective.

754

755 The release of the extract from the hybrid aerogels towards liquid media was mostly

756 a diffusion-driven process, which was strongly promoted by the highly porous

757 structure of the aerogels. In particular, the more porous structure and the greater

758 water affinity of the F2A aerogel led to a complete release of the extract in water

759 after 2-4 h. This, together with the inherent antioxidant capacity of the F2A fraction,

760 resulted in a high inhibitory effect on the β-carotene bleaching upon heating.

761 Furthermore, all the tested aerogels showed promising results to be used as bioactive

762 food packaging pads, as they were able to reduce the colour loss and lipid oxidation

763 in red meat upon refrigerated storage, being the hybrid F2A+ S-HW aerogel the most

764 active.

765

771
772
773 **References**
774
775 Barbosa-Pereira, L., Aurrekoetxea, G. P., Angulo, I., Paseiro-Losada, P., & Cruz, J.
776   M. (2014). Development of new active packaging films coated with natural

777 phenolic compounds to improve the oxidative stability of beef. *Meat Science*,
778   *97*(2), 249–254.

779 Ben Yakoub, A. R., Abdehedi, O., Jridi, M., Elfalleh, W., Nasri, M., & Ferchichi, A.
780   (2018). Flavonoids, phenols, antioxidant, and antimicrobial activities in various
781   extracts from Tossa jute leave (Corchorus olitorus L.). *Industrial Crops and*
782   *Products*, *118*(March), 206–213.

783 Benito-González, I., López-Rubio, A., & Martínez-Sanz, M. (2018). Potential of
784   lignocellulosic fractions from Posidonia oceanica to improve barrier and
785   mechanical properties of bio-based packaging materials. *International Journal*
786   *of Biological Macromolecules*, *118*, 542–551.

787 Bolumar, T., Andersen, M. L., & Orlien, V. (2011). Antioxidant active packaging for
788   chicken meat processed by high pressure treatment. *Food Chemistry*, *129*(4),
789   1406–1412.

790 Cai, J., Kimura, S., Wada, M., Kuga, S., & Zhang, L. (2008). Cellulose aerogels from
791   aqueous alkali hydroxide–urea solution. *ChemSusChem: Chemistry &*
792   *Sustainability Energy & Materials*, *1*(1□2), 149–154.

793 Camo, J., Lorés, A., Djenane, D., Beltrán, J. A., & Roncalés, P. (2011). Display life
794   of beef packaged with an antioxidant active film as a function of the
795   concentration of oregano extract. *Meat Science*, *88*(1), 174–178.

796 Carlez, A., Veciana-Nogues, T., & Cheftel, J. C. (1995). Changes in Color and
797   Myoglobin of Minced Beef Meat Due to High-Pressure Processing. *Food*
798   *Science and Technology-Lebensmittel-Wissenschaft & Technologie*, *28*(5), 528–
799   538.

800 Da Silva, A., Donoso, P., & Aegerter, M. A. (1992). Properties of water adsorbed in
801   porous silica aerogels. *Journal of Non-Crystalline Solids*, *145*, 168–174.

802 De Alencar, D. B., de Carvalho, F. C. T., Rebouças, R. H., dos Santos, D. R., dos
803   Santos Pires-Cavalcante, K. M., de Lima, R. L., … Saker-Sampaio, S. (2016).
804   Bioactive extracts of red seaweeds Pterocladiella capillacea and Osmundaria
805   obtusiloba (Floridophyceae: Rhodophyta) with antioxidant and bacterial
806   agglutination potential. *Asian Pacific Journal of Tropical Medicine*, *9*(4), 372–
807   379.

808 Dellai, A., Laajili, S., Morvan, V. Le, Robert, J., & Bouraoui, A. (2013).
809   Antiproliferative activity and phenolics of the Mediterranean seaweed
810   Laurencia obusta. *Industrial Crops and Products*, *47*, 252–255.

811 Diamante, L. M., & Lan, T. (2014). Absolute viscosities of vegetable oils at different
812   temperatures and shear rate range of 64.5 to 4835 s− 1. *Journal of Food*
813   *Processing*, *2014*.

814 Gavillon, R., & Budtova, T. (2007). Aerocellulose: new highly porous cellulose
815   prepared from cellulose− NaOH aqueous solutions. *Biomacromolecules*, *9*(1),
816   269–277.

817 Haimer, E., Wendland, M., Schlufter, K., Frankenfeld, K., Miethe, P., Potthast, A.,
818   … Liebner, F. (2010). Loading of bacterial cellulose aerogels with bioactive
819   compounds by antisolvent precipitation with supercritical carbon dioxide. In
820   *Macromolecular symposia* (Vol. 294, pp. 64–74). Wiley Online Library.

821 Heath, L., & Thielemans, W. (2010). Cellulose nanowhisker aerogels. *Green*
822   *Chemistry*, *12*(8), 1448–1453.

823 Henschen, J., Illergård, J., Larsson, P. A., Ek, M., & Wågberg, L. (2016). Contact-
824   active antibacterial aerogels from cellulose nanofibrils. *Colloids and Surfaces*

825   *B: Biointerfaces*, *146*, 415–422.

826   Hu, H., Zhao, Z., Gogotsi, Y., & Qiu, J. (2014). Compressible carbon nanotube–
827   graphene hybrid aerogels with superhydrophobicity and superoleophilicity for
828   oil sorption. *Environmental Science & Technology Letters*, *1*(3), 214–220.

829   Innerlohinger, J., Weber, H. K., & Kraft, G. (2006). Aerocellulose: aerogels and
830   aerogel□like materials made from cellulose. In *Macromolecular Symposia*
831   (Vol. 244, pp. 126–135). Wiley Online Library.

832   Jiang, F., & Hsieh, Y.-L. (2014a). Amphiphilic superabsorbent cellulose nanofibril
833   aerogels. *Journal of Materials Chemistry A*, *2*(18), 6337–6342.

834   Jiang, F., & Hsieh, Y.-L. (2014b). Super water absorbing and shape memory
835   nanocellulose aerogels from TEMPO-oxidized cellulose nanofibrils via cyclic
836   freezing–thawing. *Journal of Materials Chemistry A*, *2*(2), 350–359.

837   Jofré, A., Aymerich, T., & Garriga, M. (2008). Assessment of the effectiveness of
838   antimicrobial packaging combined with high pressure to control Salmonella sp.
839   in cooked ham. *Food Control*, *19*(6), 634–638.

840   Kannan, R. R. R., Arumugam, R., Thangaradjou, T., & Anantharaman, P. (2013).
841   Phytochemical constituents, antioxidant properties and p-coumaric acid analysis
842   in some seagrasses. *Food Research International*, *54*(1), 1229–1236.

843   Lin, J., Yu, L., Tian, F., Zhao, N., Li, X., Bian, F., & Wang, J. (2014). Cellulose
844   nanofibrils aerogels generated from jute fibers. *Carbohydrate Polymers*, *109*,
845   35–43.

846   Lorenzo, J. M., Batlle, R., & Gómez, M. (2014). Extension of the shelf-life of foal
847   meat with two antioxidant active packaging systems. *LWT - Food Science and*
848   *Technology*, *59*(1), 181–188.

849   Martínez-Abad, A., Giummarella, N., Lawoko, M., & Vilaplana, F. (2018).
850   Differences in extractability under subcritical water reveal interconnected
851   hemicellulose and lignin recalcitrance in birch hardwoods. *Green Chemistry*.

852   Martínez-Sanz, M., Erboz, E., Fontes, C., & López-Rubio, A. (2018). Valorization of
853   Arundo donax for the production of high performance lignocellulosic films.
854   *Carbohydrate Polymers*, *199*, 276–285.

855   Martínez-Sanz, M., Gómez-Mascaraque, L.G., Ballester, A.R., Martínez-Abad, A.,
856   Brodkorb, A. & López-Rubio, A. (2019). Production of unpurified agar-based
857   extracts from *Gelidium sesquipedale* seaweed by means of simplified extraction
858   protocols. *Algal Research*, *in press*.

859   Martins, C. D. L., Ramlov, F., Nocchi Carneiro, N. P., Gestinari, L. M., dos Santos,
860   B. F., Bento, L. M., … Soares, A. R. (2013). Antioxidant properties and total
861   phenolic contents of some tropical seaweeds of the Brazilian coast. *Journal of*
862   *Applied Phycology*, *25*(4), 1179–1187.

863   McMillin, K. W. (2017). Advancements in meat packaging. *Meat Science*, *132*, 153–
864   162.

865   Mulyadi, A., Zhang, Z., & Deng, Y. (2016). Fluorine-Free Oil Absorbents Made
866   from Cellulose Nanofibril Aerogels. *ACS Applied Materials and Interfaces*,
867   *8*(4), 2732–2740.

868   Nguyen, S. T., Feng, J., Le, N. T., Le, A. T. T., Hoang, N., Tan, V. B. C., & Duong,
869   H. M. (2013). Cellulose aerogel from paper waste for crude oil spill cleaning.
870   *Industrial & Engineering Chemistry Research*, *52*(51), 18386–18391.

871   Phanthong, P., Reubroycharoen, P., Kongparakul, S., Samart, C., Wang, Z., Hao, X.,
872   … Guan, G. (2018). Fabrication and evaluation of nanocellulose sponge for

873　　oil/water separation. *Carbohydrate Polymers*, *190*, 184–189.

874　Piluzza, G., & Bullitta, S. (2011). Correlations between phenolic content and
875　　antioxidant properties in twenty-four plant species of traditional ethnoveterinary
876　　use in the Mediterranean area. *Pharmaceutical Biology*, *49*(3), 240–247.

877　Rampazzo, R., Alkan, D., Gazzotti, S., Ortenzi, M. A., Piva, G., & Piergiovanni, L.
878　　(2017). Cellulose nanocrystals from lignocellulosic raw materials, for oxygen
879　　barrier coatings on food packaging films. *Packaging Technology and Science*,
880　　*30*(10), 645–661.

881　Re, Roberta., Pellegrini, Nicoletta, Proteggente, Anna., Pannala, Ananth., Yang,
882　　Min., and Rice-Evans, C. (1999). Antioxidant Activity Applying an Improved
883　　Abts Radical, *26*(98), 1231–1237.

884　Satyanarayana, K. G., Arizaga, G. G. C., & Wypych, F. (2009). Biodegradable
885　　composites based on lignocellulosic fibers—An overview. *Progress in Polymer
886　　Science*, *34*(9), 982–1021.

887　Tang, S., Sheehan, D., Buckley, D. J., Morrissey, P. A., & Kerry, J. P. (2001). Anti-
888　　oxidant activity of added tea catechins on lipid oxidation of raw minced red
889　　meat, poultry and fish muscle. *International Journal of Food Science and
890　　Technology*, *36*(6), 685–692.

891　Trache, D., Hussin, M. H., Haafiz, M. K. M., & Thakur, V. K. (2017). Recent
892　　progress in cellulose nanocrystals: sources and production. *Nanoscale*, *9*(5),
893　　1763–1786.

894　Valo, H., Arola, S., Laaksonen, P., Torkkeli, M., Peltonen, L., Linder, M. B., …
895　　Laaksonen, T. (2013). Drug release from nanoparticles embedded in four
896　　different nanofibrillar cellulose aerogels. *European Journal of Pharmaceutical
897　　Sciences*, *50*(1), 69–77.

898　Wang, X., Zhang, Y., Jiang, H., Song, Y., Zhou, Z., & Zhao, H. (2016). Fabrication
899　　and characterization of nano-cellulose aerogels via supercritical CO2 drying
900　　technology. *Materials Letters*, *183*, 179–182.

901

Highlights

• Cellulosic fractions extracted from *A. donax* biomass produced superabsorbent aerogels.

• Fractions containing hemicelluloses produced more hydrophilic and porous aerogels.

• Extracts with the highest antioxidant capacity were obtained by a heating treatment.

• Selected aerogels provided a complete release of the extract in hydrophilic media.

• Hybrid aerogels reduced oxidation processes in red meat upon storage.